ORIENTAL JOURNAL OF CHEMISTRY
An International Open Access, Peer Reviewed Research Journal
www.orientjchem.org
ISSN: 0970-020 X
CODEN: OJCHEG
2025, Vol. 41, No.(1):
Pg. 231-238

# Relative Study of Gold Nanoparticle; A Development of Green Biosensor for Detection of L-Cysteine in Urine Sample

**ROHIDAS DINKAR GOPALE[1] and RAHUL SAIDAJI DIGGIKAR[2]***

[1,2]*Department of Chemistry, New Arts, Commerce and Science College, Parner, Ahmednagar (MS), 414302, India.
*Corresponding author E-mail: diggikarrs@gmail.com

http://dx.doi.org/10.13005/ojc/410128

(Received: December 09, 2024; Accepted: January 10, 2025)

**ABSTRACT**

In this paper, we present a comparative study of bio sensing applications using gold nanoparticles (AuNPs). The AuNPs were synthesized through two distinct methods: chemical reduction and a biological approach utilizing Ocimum sanctum plant extract. In the chemical reduction method, AuNPs with an average particle size of 11.39 nm exhibited a surface plasmon resonance (SPR) peak around 527 nm. In contrast, the biological method yielded larger nanoparticles, with an average size of 17.81 nm and an SPR peak around 552 nm. The shift in wavelength correlates with the increase in particle size, which is also influenced by particle aggregation. X-ray diffraction (XRD) analysis revealed a cubic crystal structure, with the (111) plane indexed at 36.75° 2θ. Transmission electron microscopy (TEM) micrograph confirmed the uniform spherical shape of the particles synthesized by the chemical reduction method, while the biological method produced spherical particles with some size variation. The size and shape of the synthesized particles were found to be influenced by factors such as the biomolecules present in the plant extract, the pH of the solution, the volume of extract, and the temperature. The synthesized nanoparticles were incubated with biomolecules (L-cysteine, L-arginine, glycine, and ascorbic acid). Among these, only the AuNP-cysteine complex exhibited a distinct spectrometric response, with additional SPR peaks observed at 650 nm and 664 nm, confirming thiol-gold binding. The minimum detectable concentration was found to be 10 µM. Compared to the chemical reduction method, AuNPs synthesized through the biological approach demonstrated weaker thiol-gold binding, though under highly nucleophilic conditions, strong binding was observed, as indicated by the new SPR peaks. Spectroscopic methods were successfully applied for the sensitive and selective detection of cysteine in urine samples, highlighting the potential of these AuNP-based biosensors in diagnostic applications.

**Keywords:** Gold nanoparticles, Reactive species, Antioxidant, Biosensor.

## INTRODUCTION

Nanomaterials exhibit unique physical, chemical, and biological properties that make them valuable across various fields[1,2]. Due to their small size, nanomaterials possess a high surface area to volume ratio, which enhances their reactivity and makes them particularly important in optics, electronics, catalysis, and medicine. The synthesis of nanoparticles with precise size and shape control

for specific applications remains a significant challenge[3-7]. Nanoparticles (NPs) are widely used in drug delivery systems[8,16] and as biosensors, owing to their versatile properties[9-12]. Non-metallic, inorganic carbon-based NPs, in particular, have broad applications in catalysis.

In the human body, biochemical processes generate reactive oxygen species (ROS) through various reaction mechanisms. ROS includes both free radicals and non-radicals that contain active functional groups or unpaired electrons, making them highly reactive. These species are produced naturally by living organisms, and an optimal level of ROS is essential for normal cellular function. However, excessive ROS production can lead to oxidative stress, which is linked to various diseases, including cancer, chronic illnesses, and aging. ROS can damage cellular structures, including DNA, proteins, and enzymes[14-24]. Examples of ROS include hydrogen peroxide ($H_2O_2$), superoxide ($O_2^-$), hydroxyl radicals (•OH), hypochlorous acid ($ClO^-$), and singlet oxygen ($^1O_2$)[16]. Antioxidants play a crucial role in neutralizing ROS and maintaining a balance within the body. These compounds, such as glutathione (GSH), superoxide dismutase (SOD), and vitamins A, C, and E, act as reducing agents, converting harmful ROS into less damaging forms. Fruits and vegetables are rich sources of antioxidants that help minimize the risk of oxidative damage[25,36].

In this study, gold nanoparticles (AuNPs) were synthesized using two different methods: chemical reduction[4,5,36] and a biological approach involving the Ocimum sanctum plant extract. Plant-based synthesis of nanoparticles is an eco-friendly and cost-effective method, with various plants like Ocimum sanctum, Cinnamomum, Coriandrum sativum, Tamarindus indica, and Emblica officinalis used for nanoparticle production[26-35]. This biological approach is not only sustainable but also imparts additional therapeutic benefits to the nanoparticles, as the plant extracts contain bioactive compounds that assist in the reduction of metal precursors[27].

L-cysteine (Cys), an amino acid with three functional groups (-COOH, -$NH_2$, and -SH), plays a vital biological role. The thiol (-SH) group, in particular, is highly reactive and participates in nucleophilic reactions. Cysteine is an essential building block of proteins and peptides[39]. It is present in trace amounts in human body fluids, such as urine, and its deficiency is linked to kidney disorders, neurological conditions, and Alzheimer's disease[36-45]. ROS such as $H_2O_2$ and OH radicals can oxidize cysteine into cystine (a di sulphide), and an excess of cysteine can lead to cystinuria. Oxidative reactions can also impair cysteine's activity. Gold nanoparticles have shown great potential in sensing cysteine levels in biological samples, making them useful tools for health diagnostics.[37-50]

This article highlights the use of Ocimum sanctum-reduced gold nanoparticles (AuNPs) for the sensitive detection of cysteine, demonstrating their application as effective biosensors for biomolecule analysis

## MATERIALS AND METHODS

Hydrogen tetrachloroaurate (III) dehydrate ($HAuCl_4$) (Sigma-Aldrich), sodium di hydrogen phosphate ($NaH_2PO_4$) (Merck), Di-sodium hydrogen orthophosphate dehydrates ($Na_2HPO_4$) (Merck), L-Cysteine, Tri sodium citrate (Rankem), All solution prepared in doubled distilled water.

### Synthesis of gold nanoparticles

### Chemical reduction (M-I)

Gold nanoparticles (AuNPs) were synthesized through the chemical reduction of hydrogen tetrachloroaurate III ($HAuCl_4$). To begin, 10 mL of a 38.9 mM trisodium citrate solution was rapidly added to 100 mL of a 1 mM $HAuCl_4$ solution, which was then heated under reflux conditions for 15 min additional. During this process, the solution colour changed from pale yellow to red, and eventually to a deep wine red. This indicating the successful formation of AuNPs. The size of the particle depend on concentration of gold, volume of plant extract and temperature of synthesis method. The resulting mixture was allowed to equilibrate overnight at 4°C before being used in subsequent procedures.

### Biological method (M-II)

### Plant extract preparation

Fresh leaves of *Ocimum sanctum* (Tulsi) were collected from a field and thoroughly washed

with double-distilled water. The leaves were then finely chopped and placed in a conical flask. 10% (m/v) plant leaf extract prepared by mixing 10 g crushed leaves material in 100 mL double distilled water. This solution heated for 15 minutes. The resulting in a greenish-coloured solution cooled at room temperature and filtered with whatman filter paper. This plant extract were used for the synthesis of nanoparticles.

To synthesize the nanoparticles, 1 mL of 1% (v/v) the plant extract were mixed with a preheated gold solution (100 mL), and the mixture was further heated under reflux conditions for 10 minutes. During this process, the solution colour changed from pale yellow to purple. This Indicating reduction of gold ions ($Au^{III}$ to $Au^{0}$) had been completed, facilitated by the biomolecules in the plant extract. This examine phenolic compound of plant extract reduce and stabilise nanoparticle. The final concentration of gold in the nanoparticle solution was $8.72\times10^{-9}$ mol/L. The colour variation of the synthesized nanoparticles is indicative of differences in particle size. The mixture was then equilibrated overnight at 4°C for further analysis.

**Characterization**

The synthesized nanoparticles were characterized using UV-Vis double beam Spectrophotometer instrument (Analytikjena Specord 50). The absorption spectra separately recorded in 400-1100 nm range of citrate reduced gold nanoparticle and biological synthesized NPs. Transmission Electron Microscopy (TEM) analysis of the synthesized nanoparticles was performed using a high-resolution TEM (HR-TEM), JEM 2100F, at 120/200 kV at the Sophisticated Analytical Instrument Facility (SAIF), IIT Bombay. For analysis, sample droplets were deposited onto carbon-coated copper grids with a mesh size of 300 and air-dried. X-ray diffraction (XRD) patterns of AuNPs were obtained using a Bruker D8 Advanced X-ray diffract meter with Cu Kα λ = 1.5405. The data was obtained between 20-90° at 2 theta angle.

## RESULTS AND DISCUSSION

**UV-Visible spectra of AuNPs**

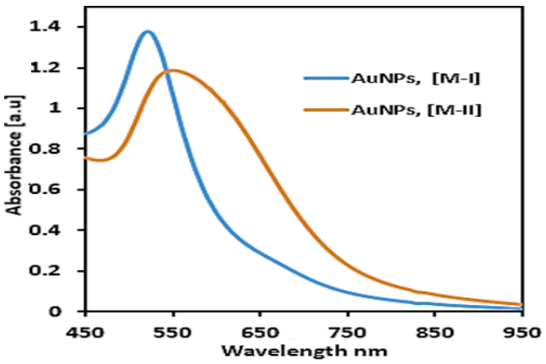


**Fig. 1. UV–Visible spectra of gold nanoparticles (AuNPs) (I) chemical reduction and (II) biological method**

SPR peak position gold nanoparticles shown in Fg. 1. AuNPs show surface plasmon resonance peak around 527 and 552 nm for chemically reduced and biological synthesized methods respectively. Sharped and intense SPR peak appears at 527 nm, for chemical method confirm spherical and uniform size of nanoparticles. In Biological synthesis, the broad peak appeared at 552 nm due to large size and variation in shape. The concentration of AuNPs determined using A = εbc, where, E extinction coefficient, b path length, c concentration of nanoparticles, A is absorption value at maximum wavelength. We found concentration of gold $3.55\times10^{-8}$ and $8.72\times10^{-9}$ mol/L respectively. The number of Au atoms attached to each nanoparticle surface calculated using given equation.

$$N_{Au} = (\pi|6)(\rho|M)D^3 \quad (1)$$

Where, D average particle size ρ is the density of Au, M atomic weight of Au. Thus, 11.39 nm sized nanoparticles composed of 42810 atoms/nanoparticles and the total number of Au atoms in 0.100 L contain $9.172\times10^{18}$ atoms/L. While 17.81 nm are sized nanoparticles composed of 174430 atoms/nanoparticles and the Total number of Au atoms in 0.100L of AuNPs solution $1.14\times10^{18}$ atoms/L. i.e. the number of Au atoms increases on the surface, as the size of particles increases. Aggregation of particles is observed in biological synthesized nanoparticles, while in chemical reduction no aggregation does not found. Intense absorption peak rises due to spherical and small size nanoparticles (no aggregation) while broad peak due to irregular shape and large size (aggregation).

**TEM of gold nanoparticles**

**Chemical reduction method(M-I)**

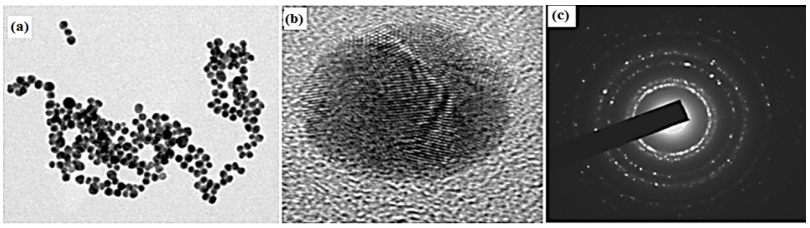


**Fig. 2(a). TEM micrograph of AuNPs (b) HR-TEM image (2nm) and C) SAED pattern of NPs**

Transmission Electron Microscopic confirm size and shape of particle. Selective area diffraction pattern highlight plane of the synthesized gold nanoparticle. Fig. 2(a) The average size of particle was found to be of the order of 11.39 nm. Considering diameter of 245 particles Fig. 3(a). SAED rings pattern show FCC structure of AuNPs and d-spacing was 0.23 nm for (220) plane Fig. 2(c). Synthesized nanoparticles are spherical. Spherical shape-controlled nanoparticles synthesis achieved at 80-90°C

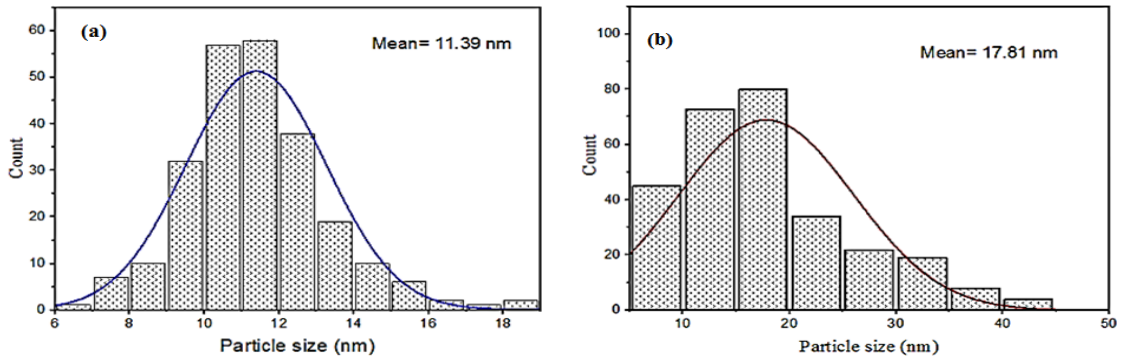


**Fig. 3. Histogram of nanoparticles (a) Chemically reduction (b) Biological synthesis**

**Biological synthesis method (M-II)**

Figure 4(a) shown TEM micrograph of gold nanoparticle. The average size of AuNPs was found to be of the order of 17.81 nm confirmed by TEM micrograph. Diameter of total 285 particles consider for observation. Fig. 3(b) Synthesized nanoparticles are spherical in shape but size not uniform. Fig.4(b) this noted that size distribution does not vary so much compare with chemical reduction. SAED rings pattern Fig. 4(c) show FCC structure of AuNPs and d-spacing was 0.24 nm for (111) plane. Synthesized nanoparticles are polycrystalline.

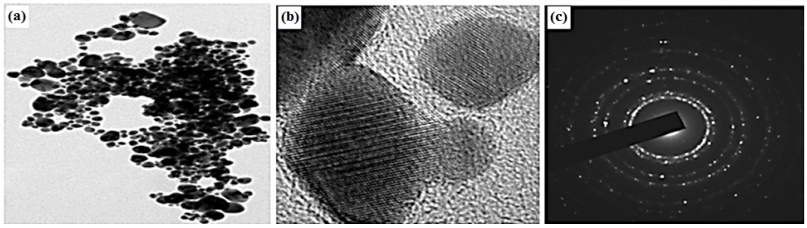


**Fig. 4(a). TEM micrograph of AuNPs (b) HR-TEM image (2nm) and C) SAED pattern of AuNPs**

**X-ray Diffraction Analysis**

Figure 5 showed XRD pattern of gold nanoparticles (AuNPs) by the chemical reduction and biological method. Intense peak of synthesized AuNPs found at 38.75°, 44.86°, 65.09°, 78.21°, 82.38° and 38.75°, 44.86°, 65.19°, 78.11°, and 82.22° indexed to (111), (200), (220), (311), (222) plane respectively. It confirms the formation of gold nanoparticles. Obtained XRD data match Jade Library Joint Committee on Powder Diffraction Standard (JCPDS) card No. 040784. Peaks observed with intensity at standard 2 theta. From experimental data, the face center cubic structure (FCC) of Au is confirmed. Average size of nanoparticle calculated using Debye- Scherrer equation.

$$D = k\lambda/\beta\cos\theta \quad (2)$$

K = constant (0.98), λ = Wavelength (1.5405 A), λ = full width at half maximum (FWHM). Average size of synthesized gold nanoparticle at intense peak found 11.39 nm for chemical reduction and 15.28 nm for biological synthesized method respectively.

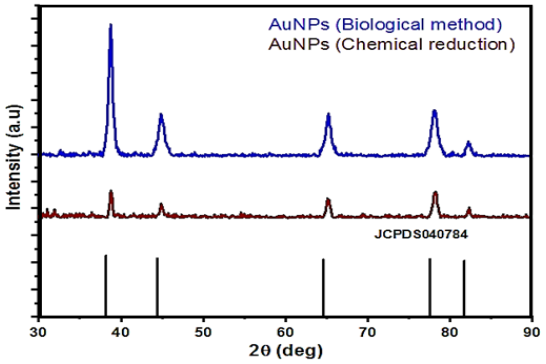


**Fig. 5. XRD pattern of gold nanoparticles**

## Selectivity of Cysteine

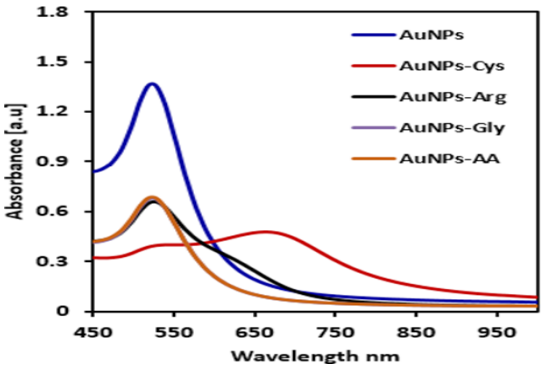


**Fig. 6. UV-Visible spectra of gold nanoparticle- Biomolecules (L-Cysteine, L-Arginine, Glycine, Ascorbic acid)**

UV-Visible spectra Fig.6 shows Surface Plasmon resonance peak for L-Cysteine, L-Arginine, Glycine, Ascorbic acid (Amino acid) incubated with gold nanoparticle (AuNPs). Only cysteine show.

The absorption spectra in Fig.7 shown an additional surface Plasmon resonance peak around 650 and 664 nm respectively, which is attributed to the binding of thiol (SH) group of cysteine to the gold nanoparticle surface. This interaction result in a specific spectral point that can be detected and analyzed. The oxidation of cysteine by hydrogen peroxide to form disulfide bonds does not show such binding. The absorption spectra in Fig. 7(b) obtained at pH 11.5 show an interaction between the cysteine and the gold nanoparticles, resulting in a peak around 664 nm. This peak indicates the binding of cysteine with nanoparticle surface.

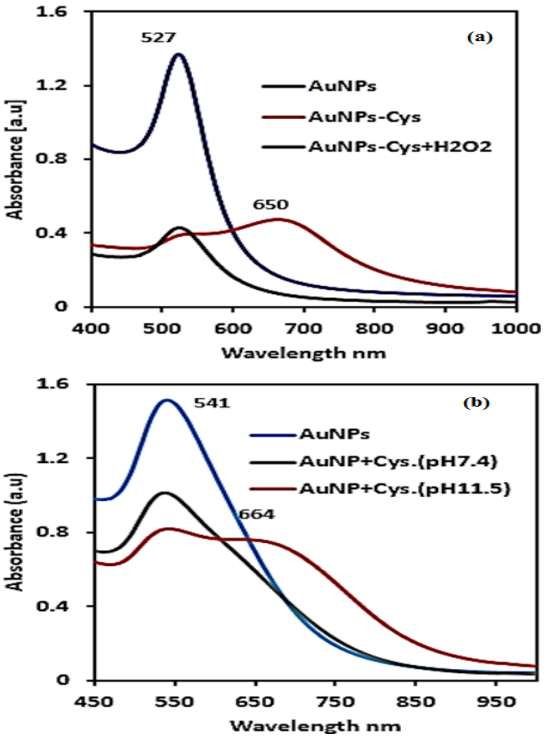


**Fig. 7. Absorption spectra of gold nanoparticle and gold nanoparticle with cysteine (a) Chemical reduction and (b) Biological synthesis**

## Study of cysteine–gold nanoparticles (Chemical method)

Different L-cysteine concentrations (ranging from 2-1000 μM) were made in a 10 mM, pH 7.4 phosphate buffer solution. 2.5 mL of gold nanoparticles (AuNPs) were mixed with 1 mL of cysteine solution and left for two hours. Nanoparticles have adsorbed L-cysteine on their surface. Gold and cysteine (SH) thiol groups exhibit binding. The nanoparticle turns from red to blue in color. This demonstrates that thiol and Au are bonded. The surface plasmon resonance peak of gold nanoparticles is located around 527 nm. The blue shift increases, and a new peak is observed at 650 nm following the addition of cysteine to the gold solution. The SPR peak shifts from 527 to 650 nm i.e. with increase in cysteine concentration strong binding noticed between SH and gold. Fig. 7 shows interaction of gold nanoparticles with cysteine.

L-cysteine concentrations vary from 2 to 1000 μM. Fig. 8(a) as concentrations of species increase, adsorption of cysteine also increases, and absorbance at the 650 nm peak appears most intense. The lowest detectable concentration of cysteine found was 10 μM.

**Sensing of cysteine from Urine sample**

0.5 mL Fresh urine sample added in 1.5 mL gold nanoparticles. After 2 h absorption spectra recorded of this reaction mixture Fig. 9. Biological method synthesized nanoparticle shows new SPR peak similar to previous reported chemical method. This new method for sensing of cysteine from urine sample and helpful for diagnosis of cysteine related problem.

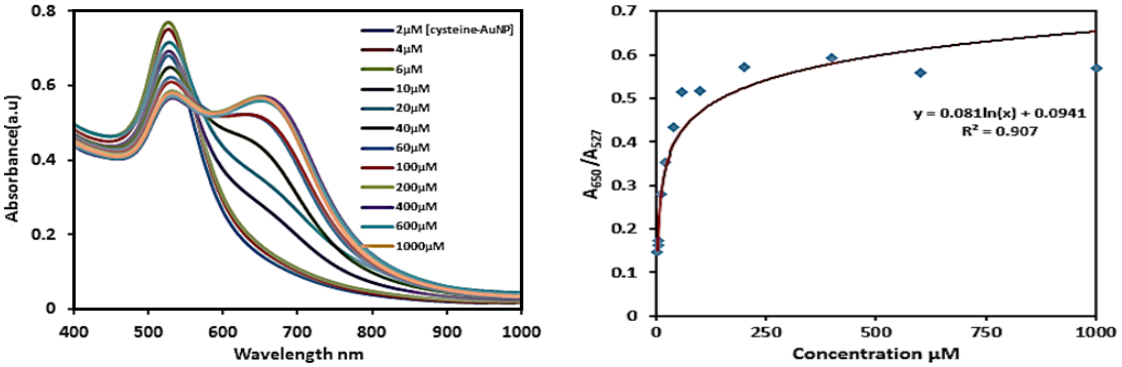


**Fig. 8. UV-Visible spectra of L-Cysteine-AuNPs (b) Absorption ratio of gold nanoparticle-cysteine at A650/A527**

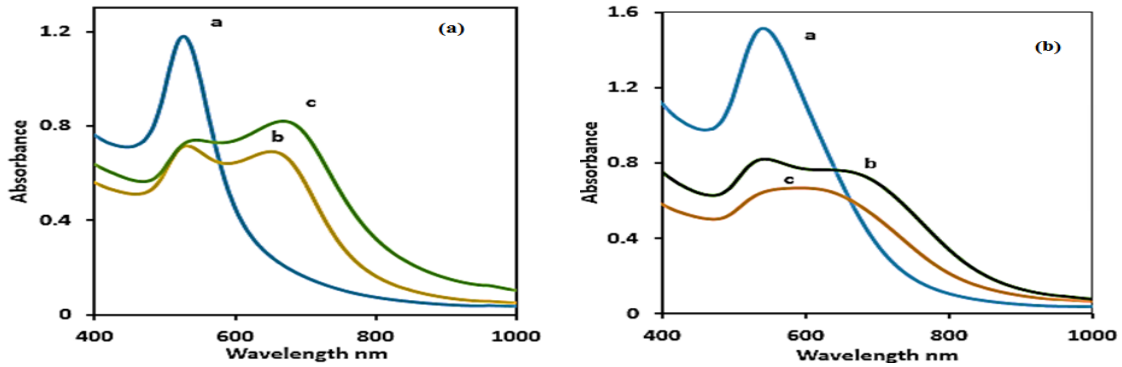


**Fig. 9. UV-Visible spectra of (a) AuNPs (b) L-Cysteine-AuNPs and c) Urine sample-AuNPs of Chemical method (a) and Biological method (b)**

## CONCLUSION

Gold nanoparticles are known for their ability to interact effectively with cysteine molecules under various physiological conditions. This study explores the potential of gold nanoparticles as a sensing tool for detecting cysteine. Gold nanoparticles reduced by Ocimum sanctum exhibit thiol-gold bonding at pH 11.5, similar to chemically synthesized gold nanoparticles. This thiol-Au bonding induces a distinct surface plasmon resonance (SPR) peak, and the characteristic wine-red color of the nanoparticles shifts to blue. When cysteine undergoes oxidation to cystine (disulfide) by hydrogen peroxide (ROS), it is unable to form the SH-Au bond, resulting in the absence of an SPR peak in the UV-Visible spectrum. Our findings suggest that biologically synthesized gold nanoparticles can be used as biomarkers for cysteine-related disorders such as cystinuria, similar to previous methods using chemically synthesized nanoparticles.

The use of biomolecule-stabilized gold nanoparticles not only enhances their medicinal properties but also makes them valuable tools for diagnostic analysis. This method is both simple and environmentally friendly, offering a sustainable approach for nanoparticle synthesis and application.

## ACKNOWLEDGEMENT

Thank full to, Sophisticated Analytical Instrument Facility (SAIF), IIT Bombay, Department of Physics, Savitribai Phule Pune University, and department of NACS College Parner for technical support

**Conflict of interest**

Author declares no conflict of interest.

**REFERENCE**


1. Das, S.; Mukherjee, A.; Sengupta, G.; Singh, V., *Elsevier*., **2020**, 371-401.
2. Herizchi, R.; Abbasi, E.; Milani, M.; Akbarzadeh. A. Artificial Cells., *Nanomedicine and Biotechnolog*., **2014**, 1–7.
3. Contini, C.; Hindley, J.; Macdonald, T.; Barritt, J.; Ces, O.; Quirke, N., *Communications Chemistry.,* **2020**, *3*, 130.
4. Xiao, Y.; Shlyahovsky, B.; Popov, I.; Pavlov, V.; Willner, I., *Langmuir*., **2005**, *21*, 5669–5662.
5. Hussain, M.; Bakar, N.; Mustapa, A.; Low, K.; Othman, N.; Adam, F., *Nanoscale Research Letters*., **2020**, *15*, 140.
6. Chen, Y. M.; Cheng, T. L.; Tseng, W. L., *Analys*., **2009**, *134*, 2106–2112.
7. Haiss, W.; Thanh, N.; Aveyard, T.; Femig, D., *Anal. Chem*., **2007**, *79*, 4215-4221.
8. Jabeen, S.; Guo, A., *International Journal of Nanomedicine*., **2020**, *15*, 9823–9857.
9. Chen, Y.; Gu, X.; Nie, C.; Jiang, Z.; Xie, Z.; Lin C., *Chem. Commun*., **2005**, 4181–4183.
10. Lin, C.; Liu, C.; Tseng, W., *Anal. Methods*., **2010**, *2*, 1810–1815.
11. Shiang, Y.; Huang C.; Chang, H., *Chem. Commun*., **2009**, 3437–3439.
12. Lee, B.; Lee, K.; Kim, I.; Park, T., *Adv. Funct. Mater*., **2009**, *19*, 1884–1890.
13. Chen, S.; Chang, H., *Analytical Chemistry*., **2004**, *76*, 3727.
14. Yang, B.; Chen, Y.; Shi., *J. Chem. Rev*., **2018**.
15. Hu, K.; Li, Y.; Rotenberg, S.; Amatore, C.; Mirkin, M., *J. Am. Chem. Soc*., **2019**, *141*, 4564–4568.
16. Hayyan, M.; Hashim, M.; AlNashef, I., *Chem. Rev*., **2016**, *116*, 3029–3085.
17. Nosaka, Y.; Nosaka A., *Chem. Rev*., **2017**, *117*, 11302-11336.
18. Wu, L.; Sedgwick, A.; Sun, X.; Bull, S.; He, X.; James, T., *Acc. Chem. Res*., **2019**, *52*, 2582–2597.
19. Burns, J.; Cooper, W.; Ferry, J.; King, D.; DiMento, B.; McNeill, K.; Miller, C.; Miller, W.; Peake, B.; Andrew, R.; Rusak, S.; Waite, T., *Aquat. Sci*., **2012**, *74*, 683–734.
20. Bhattacharya, S.; Sarkar, R.; Nandi, S.; Porgador, A.; Jelinek, R., *Anal. Chem*., **2016**.
21. Shen, Q.; Nie, Z.; Guo, M.; Zhong, C.; Lin, B.; Li W.; Yao. S., *Chem. Commun*., **2009**, 929–931.
22. Aromal, S.; Vidhu, V.; Philip, D., *Spectrochimica Acta* Part A., **2012**, *85*, 99-104.
23. Masooleh, A.; Ahmadikhah, A., *Current Analytical Chemistry*., **2020**, *16*, 112–118.
24. Liu, Z.; Ren, Z.; Zhang, J.; Chuang, C.; Kandaswamy, E.; Zhou, T.; Zuo. Li., *Frontiers in physiology*., **2018**, *9*, 477.
25. Philip D., *Elsevier*., **2009**, *73*, 650–653.
26. Gautam, P.; Kumar, S.; Tomar, M.; Singh, R.; Acharya, A.; Swaroop, S., *J Cell Sci. Ther*., **2017**, *8*, 1000278.
27. Wang, B.; Yang, G.; Chen, J.; Fang, G., *Nanomaterials*., **2020**, *10*, 1869.
28. Elia, P.; Zach, R.; Hazan, S.; Kolusheva, S.; Porat, Z.; Zeiri, Y., *International Journal of Nanomedicine*., **2014**, *9*, 4007–4021.
29. Nadaf, S.; Jadhav, N.; Naikwadi, H.; Savekar, P.; Sapkal, I.; Kambli, M., *Desai, I. Open Nano*., **2022**, *8*, 100076.
30. Muddapur, U.; Alshehri, S.; Ghoneim, M.; Mahnashi, M.; Alshahrani, M.; Khan, A.; Iqubal, S.; Bahafi, A.; More, S.; Shaikh, I.; Mannasaheb, B.; Othman N.; Maqbul, S.; Ahmad, M., *Molecules*., **2022**, *27*, 1391.
31. Teimuri-Mofrad, R.; Hadi, R.; Tahmasebi, B.; Farhoudian, S.; Mehravar, M.; Nasiri, R., *Nanochem Res*., **2017**, *2*(1), 8-19.
32. Latha, D.; Sampurnam, S.; Arulvasu, C.; Prabu, P.; Govindaraju, K.; Narayanan, V., *Materials Today: Proceedings*., **2018**, *5*, 8968–8972.
33. Akhtar, M.; Panwar, J.; Yun, Y., *ACS Sustainable Chem. Eng*., **2013**, *1*, 591–60.
34. Chandran, S.; Chaudhary, M.; Pasricha, R.; Ahmad, A.; Sastry, M., *Biotechnol. Prog*., **2006**, *22*, 577–583.
35. Nguyen, A.; Han, O.; Lim, E.; Haam, S.; Park, J.; Lee, S., *RSC Adv*., **2011**, *11*, 9664-9674.
36. Alcock, L.; Perkins, M.; Chalker., *J. Chem. Soc. Rev*., **2017.**
37. Maiti, P.; Saren, U.; Chakraborty, U.; Singha, T.; Paul, S.; Paul, P., *ACS Omeg*., **2022**, *7*, 29013–29026.
38. Acres, R.; Feyer, V.; Tsud, N.; Carlino, E.; Prince, K., *J. Phys. Chem*., **2014**, *118*, 10481–10487.
39. Aryal, S.; B.K.C, R.; Dharmraj, N.; Bhattarai, N.; Kim, Chi.; Kim, H., *Spectrochimica Acta* Part A., **2006**, *63*, 160–163.

40. Luo, D.; Smith, S.; Anderson, B., *Journal of Pharmaceutical Sciences*., **2016**, *94*, 304–316.
41. Petean, I.; Tomoaia, GH.; Horovitz, O.; Mocanu, A.; Tomoala-cotisel, M., *Journal of Optoelectronics and Advanced Materials*., **2008**, *10*(9), 2289–2292.
42. Garda-Santamarina, S.; Boronat, S.; Hidalgo, E., *Biochemistry*., **2014**, *53*, 2560–2580.
43. Burgos, R.; Fontmorin, M.; Tang, Z.; Benetton X.; Sillanpaa, M., *RSC Adv*., **2018**, *8*, 5321–5330.
44. Jeong, M.; Yu, K.; Chung, H.; Park, S.; Lee, A.; Song, M.; Cho, M.; Kim., *J. Scientific Reports*., **2016**, *6*, 26347.
45. Saha, K.; Agasti, S.; Kim, C.; Li, X.; Rotello, V., *Chemical Reviews*., **2012.**
46. Li, Li.; Li, B., *Analyst*., **2009**, *134*, 1361-1365.
47. Rehman, T.; Shabbir, M.; Raheem, M.; Manzoor, M.; Ahmad, N.; Liu, Z., *Food Sci Nutr*., **2020**, *8*, 4696-4707.
48. Chen, Z.; Luo, S.; Liu, C.; Cai, Q., *Anal Bioanal Chem*., **2009**, *395*, 489-494.
49. Wu, H.; Huang C.; Cheng, T.; Tseng, W., *Talanta*., **2008**, *76*, 347-352.
50. Mocanu, A.; Cernica, I.; Tomoaia, G.; Bobos, L.; Horovitz, O.; Cotisel, M., *Colloids and Surfaces A: Physicochem Eng. Aspects*., **2009**, *3(*38), 93-101.